HHS Public Access

Author manuscript

Circ Heart Fail. Author manuscript; available in PMC 2019 January 01.

Published in final edited form as:

Circ Heart Fail. 2018 January ; 11(1): e004313. doi:10.1161/CIRCHEARTFAILURE.117.004313.

Novel Wearable Seismocardiography and Machine Learning Algorithms Can Assess Clinical Status of Heart Failure Patients

Omer T. Inan, PhD[1,†], **Maziyar Baran Pouyan, PhD**[1,†], **Abdul Q. Javaid, PhD**[1], **Sean Dowling**[2], **Mozziyar Etemadi, MD, PhD**[3], **Alexis Dorier**[1], **J. Alex Heller, MS**[3], **A. Ozan Bicen, PhD**[1], **Shuvo Roy, PhD**[2], **Teresa De Marco, MD**[2], and **Liviu Klein, MD**[2]

[1]Georgia Institute of Technology, Atlanta, GA

[2]University of California, San Francisco, CA

[3]Northwestern University, Chicago, IL

Abstract

Background—Remote monitoring of heart failure (HF) patients using wearable devices can allow patient-specific adjustments to treatments and thereby potentially reduce hospitalizations. We aimed to assess HF state using wearable measurements of electrical and mechanical aspects of cardiac function in the context of exercise.

Methods and Results—Patients with compensated (outpatient) and decompensated (hospitalized) HF were fitted with a wearable electrocardiogram (ECG) and seismocardiogram (SCG) sensing patch. Patients stood at rest for an initial recording, performed a six-minute walk test (6MWT), and then stood at rest for five minutes of recovery. The protocol was performed at the time of outpatient visit or at two time points (admission and discharge) during an HF hospitalization. To assess patient state, we devised a method based on comparing the similarity of the structure of SCG signals following exercise compared to rest using graph mining (Graph Similarity Score, GSS). We found that GSS can assess HF patient state, and correlates to clinical improvement in 45 patients (13 decompensated, 32 compensated). A significant difference was found between the groups in the GSS metric (44.4±4.9 [Decompensated HF] vs. 35.2±10.5 [Compensated HF], $p<0.001$). In the six decompensated patients with longitudinal data we found a significant change in GSS from admission (decompensated) to discharge (compensated) (44±4.1 [Admitted] vs. 35±3.9 [Discharged], $p<0.05$).

Conclusions—Wearable technologies recording cardiac function and machine learning algorithms can assess compensated and decompensated HF states by analyzing cardiac response to sub-maximal exercise. These techniques can be tested in the future to track the clinical status of outpatients with HF and their response to pharmacological interventions.

Corresponding Author: Omer T. Inan, PhD, Georgia Institute of Technology, Technology Square Research Building, 85 Fifth St. NW, Suite TSRB 417, Atlanta, GA, 30308, inan@gatech.edu, phone: 404-385-1724.

†Both authors contributed equally and should be considered first author.

Disclosures

O. T. Inan has consulting/advisory board relationships with Physiowave, Inc. Other authors have no significant relationships to disclose.

Keywords

Wearable technology; Graph similarity score; Heart failure monitoring

Subject Codes

Heart Failure; Hemodynamics; Exercise Testing; Contractile Function

Heart failure (HF) affects 6.5 million Americans and contributes to nearly 300,000 deaths per year[1]. There are more than 1 million hospital discharges for HF annually and, although many efforts have been made to reduce these hospitalizations, the number has remained relatively constant over the past decade[1]. Moreover, following hospitalization, nearly one fourth of all HF patients are readmitted within 30 days, and at least half of these readmissions are due to HF[2]. Such hospitalizations greatly impact mortality rates, with the risk of death increasing significantly following hospitalization, and more so with longer duration of hospitalization or repeat hospitalization[3].

The most common factor associated with HF-related hospitalizations is congestion[4, 5] due to elevated left ventricular filling pressures[6, 7], leading to symptoms such as dyspnea, edema, and fatigue that usually occur only a few days before hospitalization[8]. While treatment during hospitalization reduces signs and symptoms of congestion, even at discharge nearly half of HF patients still show such signs and, in fact, this subset of patients has been demonstrated to be at a significantly higher risk of readmission and long term mortality[9, 10]. Accordingly, the monitoring of HF patients after discharge to proactively manage their care has been recognized as an important need[11], and multiple tools have been developed and evaluated for this purpose.

Approaches for outpatient HF monitoring have included daily weight measurements and telemonitoring of patient-reported symptoms and vital signs[12, 13], natriuretic peptides[14], non-invasive bioimpedance monitors[15], implantable bioimpedance monitors[16, 17], and implantable hemodynamic sensors[18–20]. Other than the direct measurement of intracardiac filling pressures using implantable sensors, none of these approaches has successfully shown improvement in outcomes for HF patients in large randomized controlled trials. Unfortunately, implantable pressure sensors are invasive, hampering patients' enthusiasm for their use, and the cost of each implant is more than $20,000. Thus, there are millions of HF patients worldwide that still lack an effective solution for adequate, remote proactive care.

A non-invasive and inexpensive alternative capable of measuring relevant hemodynamic parameters associated with HF worsening could significantly advance home HF management. However, there is no tool available for non-invasive measurement of filling pressures and, thus, a more indirect approach must be designed.

We propose wearable measurements of cardiovascular hemodynamics before and after a controlled "dosage" of exercise – the six minute walk test (6MWT)[21, 22] – as a means of non-invasively assessing hemodynamic changes at home[23]. Specifically, we measure the seismocardiogram (SCG) signal, which represents the vibrations of the chest wall in

response to the movement of blood through the arterial tree, and the movement of the heart in the chest[24, 25]. The SCG consists of waves in the time domain that have been shown, using echocardiography as a reference standard, to correspond to aortic valve opening and closing events, as well as the rapid ejection of blood into the aorta[25]. In healthy subjects, exercise leads to substantial changes in the shape and timings of the waveform: for example, the shortening isovolumetric contraction time associated with increased sympathetic tone compresses the SCG waves in time and thus increases the high frequency components[26]. Our main hypothesis was that the changes in the signal associated with the 6MWT would be significantly less for decompensated HF patients as compared to compensated patients, since the decompensated patients have less cardiovascular reserve to increase their cardiac performance in response to the exercise challenge.

Changes in intracardiac filling pressures relate to changes in stroke volume in order to maintain the Frank-Starling curve, and therefore assessing changes in cardiac contractility can give an indirect assessment of intracardiac filling pressures[27]. Exertional intolerance is a hallmark of both HF with reduced and preserved ejection fraction, and is known to worsen as a patient's condition progresses. One proposed mechanism for the exertional intolerance is the lack of cardiovascular reserve, as demonstrated in studies where HF patients were unable to increase cardiac output with dobutamine infusion[28]. With worsening hemodynamic congestion, the beta-receptors are down regulated, and the sensitivity of the myocardial responsiveness to beta stimulation is blunted; thus, during a stressor (i.e., exercise), myocardial contractility cannot be increased successfully to meet the increased body demands.

In this work, we aimed to derive a non-invasive physiological biomarker related to cardiovascular reserve for patients with HF that could be quantified based on wearable SCG measurements. Specifically, we developed an analytic graph-mining-based approach to measure spectral domain similarity of SCG signals before and after a 6MWT using a wearable patch to provide a non-invasive assessment of the intracardiac hemodynamic changes related to the HF state.

Methods

The data that support the findings of this study are available from the corresponding author upon reasonable request.

Wearable Patch Hardware

Unlike impedance based measurements, SCG is not confounded by fluid shifts in the body and does not require the application of a large number of electrodes on the chest. We measure the SCG signal using a custom wireless patch[26] mounted at the mid-sternum that includes an ultra-low noise tri-axial accelerometer to capture the three components of the signal: dorso-ventral, head-to-foot, and lateral accelerations, as shown in Figure 1. The chest vibrations produce a repeatable signal shape that includes peaks corresponding to key events of the cardiac cycle.

The wearable patch (7 cm diameter × 1 cm thickness, 40 g weight) is mounted to the patient's chest mid-way between the suprasternal notch and the xiphoid process using three Ag/AgCl adhesive-backed gel electrodes (Red Dot 2560, 3M, Maplewood, MN). The patch includes electronics for measuring ECG signals from these electrodes, as well as SCG signals using a tri-axial microelectromechanical systems (MEMS) based accelerometer (BMA280, Bosch Sensortec GmbH, Reutlingen, Germany). The data from these sensors are sampled at 500 Hz and stored on a micro secure digital (microSD) card. The overall battery life of the system is 50 hours between charge cycles, thus allowing 24-hour around-the-clock recording including possibly during sleep. The combination of very high-resolution acceleration measurements from the chest to facilitate high quality wearable SCG signal capture and extended battery life to enable long-term monitoring was enabled by cutting edge embedded systems hardware and firmware design. A detailed description of the patch design and validation has been previously described.[26]

Study Protocol

Under a protocol approved by the University of California, San Francisco and Georgia Institute of Technology Institutional Review Boards, patients with HF were enrolled from the outpatient HF clinic or from the inpatient Cardiology service: the patients were stage C, not stage D advanced HF patients. There were no restrictions in terms of ejection fraction, renal function or use of intravenous medications (including inotropes) for this study. Patients were classified as compensated or decompensated based on the individual clinician assessment, which was derived from patient symptoms and physical exam findings (summarized in Table 1). The compensated patients were assessed at the time of the outpatient clinic visit, while the decompensated patients were assessed on the day of admission during their hospitalization before effective decongestive treatments had been used. Six decompensated patients had the measurements performed both shortly after admission and on the day of discharge.

Upon providing written informed consent, each subject was fully characterized based on echocardiography, serum biomarkers, symptoms, and medical history. The wearable patch was affixed to each subject's sternum, and after an initial 60 seconds of rest, baseline physiological measurements were obtained. Following these measures, the subject performed a 6MWT, where the standard protocol was followed by the study coordinator in terms of describing the procedure to the patient and observing the test[29]. The distance walked by the subject was measured, and converted to a percent predicted 6MWT distance[29]. After completing the 6MWT, the subject was asked to stand still for 5 minutes (recovery phase) as the physiological data were measured using the wearable patch.

Non-Invasive Physiological Biomarker Quantification

The main goal of proposed methodology is to quantify the spectral domain similarity between the measured SCG signal (as a surrogate of cardiovascular hemodynamics and cardiac contractility) before and after a 6MWT. We expect that the quantified similarity can allow for phenotyping of patients with HF as compensated or decompensated. Conventional approaches to such a problem typically involve extracting time intervals or amplitude measurements from the SCG signals before and after exercise and quantifying the changes

in the waveform associated with the 6MWT. However, such approaches can be confounded by noise, since they rely on the accurate detection of particular features in the signal, rather than examination of underlying structural characteristics of the signal. The novel methodology we are proposing here involves two main steps: (1) Pre-Processing and Feature Extraction, and (2) Graph Similarity Computation. By computing the similarity score from the graph representing the structure of the data in the spectral domain, we anticipate that a more robust biomarker can be extracted from the physiological data. The overall workflow for the proposed approach is presented in Figure 2.

Pre-Processing and Feature Extraction

For pre-processing the signals, first linear filtering was applied on the captured SCG to reduce out-of-band noise (bandwidth: 0.8 – 35 Hz [ECG and dorso-ventral SCG], and 0.8 – 20 Hz [lateral and head-to-foot SCG]). These filter bandwidths were selected such that low frequency baseline wander due to respiration and higher frequency noise and artifacts associated with valve closure acoustics were removed from the signals, while still preserving the key morphological features of the SCG. The extracted waveforms from each axis were then averaged to obtain traces with attenuated movement artifacts and uncorrelated noise (Figure 2(a)). While such averaging across axes removes the possibility of extracting axis-specific information from the SCG signal, the focus in this paper was to reduce the noise to the extent possible and fuse the three axes into the overall graph-based analytics accordingly.

For each subject, the filtered (and averaged) SCG signal (SCG_{3D}) of rest and recovery (for the first 60 seconds) were extracted and separated. Next, we normalized both signals to follow a distribution with zero mean and unity variance. This mitigates any differences in signal amplitude that may result from variability in mechanical coupling of the sensing system to the chest from person to person, or moderate compromise in the interface following exercise due to sweating and slight changes in the electrode adhesion. The normalized signals were then segmented using a window size of 1000 ms with 50% overlap, resulting in N_{RES} and N_{REC} segmented windows from the Rest (*RES*) and Recovery (*REC*) phases, respectively. Note that the considered window size was selected heuristically to allow for any cardiovascular signatures to be present within a given window.

Next, we computed the Fourier Transform[30] on each window of N_{RES}. The absolute value of the frequency domain components in different frequency bands were considered as features for each window. For each frequency band, the median of extracted features through all the windows were calculated. This generated a feature vector $\boldsymbol{X} = \{x_1, x_2, \ldots, x_N\}$ (where i indicates i_{th} band and N denotes the number of frequency bands) representing the spectral characteristics of the entire N_{RES}. Finally, we applied the same feature extraction approach to calculate the frequency domain features $\boldsymbol{Y} = \{y_1, y_2, \ldots, y_N\}$ from N_{REC} (Figure 2(b)).

Graph Similarity Score Computation

To quantify structural changes in the SCG signal before and after a 6MWT (rest and recovery phases), we computed the similarity between the extracted feature vectors $\boldsymbol{X}$ and $\boldsymbol{Y}$. Although there are several traditional techniques such as Minkowski and correlation-based similarity scores[31] to measure similarity, all of them have two major drawbacks: (i) their

practical efficiency reduces by increasing vector dimensionality due to the curse of dimensionality[32] (i.e. a phenomenon in high dimensional space which prevents common data organization to be effective); and (ii) they do not consider pertinent dependencies among measured features. Therefore, to overcome these challenges, we employed an approach that is commonly used in graph theory. We modeled each feature vector using a k-Nearest Neighbor Graph (kNNG)[33], then calculated structural similarity between these graphs using a simple graph matching approach. This method overcomes the related drawbacks to the traditional techniques as it models possible dependencies among frequency features using a network structure. We used a value of k = 20, but also computed the results with k = 10 and 30 without any substantial differences in the final results.

We used both feature vectors $\boldsymbol{X}$ and $\boldsymbol{Y}$ to construct two kNNG graphs per subject (G_X and G_Y). An important benefit of the graph mining is that the feature vectors can be readily visualized in lower-dimensional (i.e., 2D) space while preserving the underlying geometric relationships between the features. We represent the features of $\boldsymbol{X}$ as vertices in the graph and connect each vertex to its k nearest neighboring vertices using Euclidean distance. This process makes an unweighted-undirected graph G_X from $\boldsymbol{X}$. The same process is performed to extract G_Y from Y (Figure 2(c)).

Finally, we count the number of common edges that exist in both graphs and consider that as a structural similarity between two graphs. In this paper, we refer to this as the Graph Similarity Score (GSS). Unlike traditional techniques, GSS is able to capture the structural similarity of the SCG signal between rest and recovery phases, since it considers possible dependencies of features using applied graph mining. Figure 2(d) shows a simple example of GSS calculation using two illustrative graphs. In this example, the GSS between the two graphs is four, since four common edges exist between them.

Statistical Analysis

The calculated GSS between rest and recovery phases for the decompensated versus compensated patients were compared using the Mann-Whitney U test. Additionally, the Wilcoxon signed-rank test was used to compare the changes in GSS for the patients with HF from admit to discharge (longitudinal study). The demographics of patients in the decompensated and compensated groups were compared using Student's t-test. The 6MWT walking distances, percent predicted walking distances, and heart rates for the patients with HF from admit to discharge (longitudinal study) were compared using a paired t-test. Means are expressed as mean ± standard deviation.

Results

Of the 45 subjects enrolled in the study, 13 were decompensated hospitalized [ejection fraction (EF): 0.24 ± 0.11] and 32 were compensated ambulatory (EF: 0.35 ± 0.15) HF patients. There were no significant baseline differences between the groups in terms of demographics (i.e., age, height, and weight, $p > 0.05$ based on Student's t-test).

The GSS is significantly higher in decompensated than in compensated HF patients, suggesting a reduced cardiovascular reserve for decompensated patients

Figure 3 shows representative SCG ensemble averages from rest and immediately following the 6MWT (recovery phase), and related G_X and G_Y graphs of a decompensated patient with HF (bottom) and a compensated patient (top). For the decompensated patient, the GSS value between G_X and G_Y is 55 and for the compensated patient the calculated GSS value is 24. This result indicates the higher similarity in contractility and cardiovascular hemodynamics between rest and recovery phases for decompensated patients in comparison with compensated patients.

These single subject representative results are consistent with the overall findings from all participants, summarized in Figure 4 (compensated versus decompensated). The calculated GSS values were significantly higher for the decompensated compared to compensated patients: 44.4 ± 4.9 vs. 35.2 ± 10.6, respectively, $p<0.01$.

To understand the effects of the time duration during recovery (nominally selected as 60 seconds in this paper) that is selected at the “recovery phase” to then compare against the “rest phase,” we recalculated the GSS metric with varying durations of the recovery phase for all the subjects and computed corresponding p-values. The best result (most significant value) was found when the initial one minute of recovery was compared with rest phase. Incorporating a longer time interval (e.g. 5 minutes) after the 6MWT reduces the differences between the decompensated and compensated groups, since the cardiovascular system recovers back to the resting state for both groups of patients following exercise after a few minutes.

The absolute and percent predicted 6MWT distance were significantly higher for the compensated compared to decompensated patients: 369 m ± 102 m vs. 250 m ± 130 m for the compensated and decompensated patients, respectively, $p < 0.01$; and 71% ± 25% vs. 41% ± 20%, for the compensated and decompensated, respectively, $p < 0.01$.

We computed GSS across NYHA Class for all subjects, and we found a monotonic increase with respect to class. Patients with NYHA Class I-IV symptoms had the following GSS values: 24.3 ± 4.3, 36.8 ± 11.4, 37 ± 10, and 42.5 ± 6.0. Statistical significance was only found in the differences between Class I and all other classes.

GSS in treated decompensated HF patients decreases from admission to discharge, indicating improvement in cardiovascular reserve

Figure 5 depicts results from the subset of decompensated HF patients that participated in two sessions (longitudinal cases). The GSS between the rest and recovery phases was significantly higher on admission compared to discharge: 44 ± 4.1 [admitted] vs. 35 ± 3.9 [discharged], $p<0.05$. Additionally, one patient had a third visit as well. As presented in Figure 5, that patient had an increased GSS in the third visit because of readmission due to acute kidney injury and associated volume overload.

For these same patients, the absolute and percent-predicted 6MWT distance also increased from 90.9 m ± 48.1 m to 115.5 m ± 37.3 m ($p = 0.33$) and 30% ± 19% to 36% ± 16% ($p =$

0.08), respectively, but the increases were not significant. The changes in heart rate in response to the 6MWT exercise increased slightly from admit to discharge (12.2 bpm ± 10.6 bpm to 13.5 bpm ± 11.6 bpm, p = 0.66) but these increases were also not significant.

Discussion

We have presented data demonstrating that a small, lightweight wearable patch for measuring changes in GSS in response to a controlled exercise protocol can differentiate between decompensated and compensated HF patients. The results are consistent with physiological expectations: the decompensated (and more congested) patients have less cardiovascular reserve, and thus are not able to modulate their hemodynamics or cardiac contractility as effectively as the compensated patients during exercise. Importantly, for the one patient that was readmitted with abnormal volume status a higher value of GSS (indicating reduced cardiovascular reserve) was found. For the longitudinal study evaluating within-subject improvements from admission to discharge, the calculated GSS showed a significant improvement (decreasing in GSS value) with treatment, while other factors such as heart rate response to exercise, 6MWT distance, and percent-predicted distance did not show significant improvement. This result suggests that the GSS metric may be more sensitive to changes in patient status than these other more traditional measures of the responses of the cardiovascular system to exercise. Since the 6MWT distance itself has already been validated as a prognostic for patients with HF, these results are promising and motivate further studies for evaluating the technology in larger populations of patients with HF.

While beta blockers impact cardiac contractility and thus might affect the SCG data, the differences in total beta blocker use were not significantly different between the two groups studied (decompensated and compensated patients). A total of 77% of the decompensated and 90% of the compensated patients were using beta blockers. Thus, we do not expect that the GSS differences between the two groups were confounded by beta blocker use. Future studies should analyze the effects of beta blocker dosage on SCG data and GSS.

Since the proposed graph analytic technique works based on multiple extracted features from the SCG signal, it is more robust to motion artifacts, day-to-day variability, and noise compared to conventional peak detection approaches. This machine learning algorithm can also potentially be implemented in a real-time monitoring system to evaluate the status of HF patients, as its time complexity is very low. Indeed, the concept of using graph analytics as compared to single features of physiological signals can be applied more broadly to other cardiovascular signals as well, such as impedance cardiogram or photoplethysmogram waveforms. Conventional feature extraction approaches rely on the accurate detection of peaks in the time or frequency domain, and these peaks can often be corrupted by motion artifacts and other disturbances in practical recordings outside of lab or clinical settings. Tracking changes in the signals in the feature space, as enabled by GSS for example, reduces the burden on the extraction methods for each individual feature, as the overall cloud of features is tracked in high-dimensional space rather than a single feature alone.

The research has several limitations that should be noted. Currently, the differentiation between the groups (compensated and decompensated) was not sufficiently large to facilitate classification of patient state; future work will be needed to enhance the ability of the algorithms to perform such classification. The approach requires the patient to perform a 6MWT and to stand still for at least 60 seconds before and after the test, which may be inconvenient. Nevertheless, such a procedure may only be required once per day or every other day, and it is possible that in future studies a less obtrusive stressor may be employed while still preserving the accuracy of the derived features. In future work, we will investigate such approaches and define a “dose response” curve for decompensated and compensated patients relating GSS changes to activity “dosage” (e.g., in units of estimated energy expenditure, distance walked, or time walked). Another limitation is the relatively small population of patients in the longitudinal study. While significant results were obtained, the number of participants is small and must be expanded in future studies to better evaluate the potential advantage of this approach compared to heart rate and activity monitors. Specifically, this small single center study will require replication in larger prospective trials in multiple sites. An important characteristic of the patch system described here is that, in addition to hemodynamic measurements, high quality ECG-based heart rate and rhythm and accelerometer-based activity data are also inherently collected. Thus, the SCG-derived features are supplementing existing technologies rather than attempting to replace them, providing the opportunity for fused metrics of improving or worsening condition using a single wearable device. Additionally, the compensated/decompensated status of each patient was known to the investigators since this was a first proof-of-concept study; future studies should employ a blinded assessment to determine if GSS can predict clinical status. Finally, the measurements described in this paper were obtained in a controlled, clinical environment only, and the results at home in unsupervised settings may be of lower quality than the data obtained here. In future work, the wearable patch will be tested in patients at home to determine whether markers of increasing congestion can be successfully derived towards ultimately titrating care based on the non-invasive physiological measurements from the system.

Conclusions

We have shown that a wearable device capable of recording electrical and mechanical aspects of cardiac function and graph mining techniques analyzing cardiac response to sub-maximal exercise can be used to identify compensated and decompensated HF states and to track the clinical course of the patients. These techniques can be tested in the future to track the clinical status of outpatients with HF and their response to pharmacological interventions.

Acknowledgments

Sources of Funding

Research reported in this publication was supported in part by the National Institute on Aging under Award Number R56AG048458, and the National Heart, Lung and Blood Institute under R01HL130619. The content is solely the responsibility of the authors and does not necessarily represent the official views of the National Institutes of Health.

References

1. Benjamin EJ, Blaha MJ, Chiuve SE, Cushman M, Das SR, Deo R, de Ferranti SD, Floyd J, Fornage M, Gillespie C, Isasi CR, Jiménez MC, Jordan LC, Judd SE, Lackland D, Lichtman JH, Lisabeth L, Liu S, Longenecker CT, Mackey RH, Matsushita K, Mozaffarian D, Mussolino ME, Nasir K, Neumar RW, Palaniappan L, Pandey DK, Thiagarajan RR, Reeves MJ, Ritchey M, Rodriguez CJ, Roth GA, Rosamond WD, Sasson C, Towfighi A, Tsao CW, Turner MB, Virani SS, Voeks JH, Willey JZ, Wilkins JT, Wu JHY, Alger HM, Wong SS, Muntner P. Heart Disease and Stroke Statistics—2017 Update: A Report From the American Heart Association. Circulation. 2017; 135:e146–e603. [PubMed: 28122885]
2. Dharmarajan K, Hsieh AF, Lin Z, Bueno H, Ross JS, Horwitz LI, Barreto-Filho JA, Kim N, Bernheim SM, Suter LG, Drye EE, Krumholz HM. Diagnoses and timing of 30-day readmissions after hospitalization for heart failure, acute myocardial infarction, or pneumonia. JAMA. 2013; 309:355–363. [PubMed: 23340637]
3. Solomon SD, Dobson J, Pocock S, Skali H, McMurray JJV, Granger CB, Yusuf S, Swedberg K, Young JB, Michelson EL, Pfeffer MA. Influence of nonfatal hospitalization for heart failure on subsequent mortality in patients with chronic heart failure. Circulation. 2007; 116:1482–1487. [PubMed: 17724259]
4. Fonarow GC. The Acute Decompensated Heart Failure National Registry (ADHERE): opportunities to improve care of patients hospitalized with acute decompensated heart failure. Rev Cardiovasc Med. 2003; 4(Suppl 7):S21–30.
5. Cleland JGF, Swedberg K, Follath F, Komajda M, Cohen-Solal A, Aguilar JC, Dietz R, Gavazzi A, Hobbs R, Korewicki J, Madeira HC, Moiseyev VS, Preda I, van Gilst WH, Widimsky J, Freemantle N, Eastaugh J, Mason J. The EuroHeart Failure survey programme—a survey on the quality of care among patients with heart failure in Europe. Eur Heart J. 2003; 24:442–463. [PubMed: 12633546]
6. Adamson PB, Magalski A, Braunschweig F, Böhm M, Reynolds D, Steinhaus D, Luby A, Linde C, Ryden L, Cremers B, Takle T, Bennett T. Ongoing right ventricular hemodynamics in heart failureclinical value of measurements derived from an implantable monitoring system. J Am Coll Card. 2003; 41:565–571.
7. Zile MR, Bennett TD, StJohn Sutton M, Cho YK, Adamson PB, Aaron MF, Aranda JM, Abraham WT, Smart FW, Stevenson LW, Kueffer FJ, Bourge RC. Transition from chronic compensated to acute decompensated heart failure. Circulation. 2008; 118:1433–1441. [PubMed: 18794390]
8. Gattis WA, O'Connor CM, Gallup DS, Hasselblad V, Gheorghiade M. Predischarge initiation of carvedilol in patients hospitalized for decompensated heart failure. Results of the initiation management predischarge: process for assessment of carvedilol therapy in heart failure (IMPACT-HF) trial. J Am Coll Card. 2004; 43:1534–1541.
9. Ambrosy AP, Pang PS, Khan S, Konstam MA, Fonarow GC, Traver B, Maggioni AP, Cook T, Swedberg K, Burnett JC, Grinfeld L, Udelson JE, Zannad F, Gheorghiade M. Clinical course and predictive value of congestion during hospitalization in patients admitted for worsening signs and symptoms of heart failure with reduced ejection fraction: findings from the EVEREST trial. Eur Heart J. 2013; 34:835–843. [PubMed: 23293303]
10. Zile MR, Bennett TD, El Hajj S, Kueffer FJ, Baicu CF, Abraham WT, Bourge RC, Stevenson LW. Intracardiac pressures measured using an implantable hemodynamic monitor: relationship to mortality in patients with chronic heart failure. Circ Heart Fail. 2017; 10:3594–3602.
11. Bui AL, Fonarow GC. Home monitoring for heart failure management. J Am Coll Card. 2012; 59:97–104.
12. Chaudhry SI, Wang Y, Concato J, Gill TM, Krumholz HM. Patterns of weight change preceding hospitalization for heart failure. Circulation. 2007; 116:1549–1554. [PubMed: 17846286]
13. Ong MK, Romano PS, Edgington S, Aronow HU, Auerbach AD, Black JT, De Marco T, Escarce JJ, Evangelista LS, Hanna B, Ganiats TG, Greenberg BH, Greenfield S, Kaplan SH, Kimchi A, Liu H, Lombardo D, Mangione CM, Sadeghi B, Sadeghi B, Sarrafzadeh M, Tong K, Fonarow GC. Better Effectiveness After Transition - Heart Faliure (BEAT-HF) Research Group. Effectiveness of remote patient monitoring after discharge of hospitalized patients with heart failure: The Better Effectiveness After Transition - Heart Failure (BEAT-HF) randomized clinical trial. JAMA Intern Med. 2016; 176:310–318. [PubMed: 26857383]

14. Felker GM, Ahmad T, Anstrom KJ, Adams KF, Cooper LS, Ezekowitz JA, Fiuzat M, Houston-Miller N, Januzzi JL, Leifer ES, Mark DB, Desvigne-Nickens P, Paynter G, Piña IL, Whellan DJ, O'Connor CM. Rationale and Design of the GUIDE-IT StudyGuiding Evidence Based Therapy Using Biomarker Intensified Treatment in Heart Failure. JACC: Heart Failure. 2014; 2:457–465. [PubMed: 25194287]
15. Packer M, Abraham WT, Mehra MR, Yancy CW, Lawless CE, Mitchell JE, Smart FW, Bijou R, O'Connor CM, Massie BM, Pina IL, Greenberg BH, Young JB, Fishbein DP, Hauptman PJ, Bourge RC, Strobeck JE, Murali S, Schocken D, Teerlink JR, Levy WC, Trupp RJ, Silver MA. Utility of impedance cardiography for the identification of short-term risk of clinical decompensation in stable patients with chronic heart failure. J Am Coll Card. 2006; 47:2245–2252.
16. Yu C-M, Wang L, Chau E, Chan RH-W, Kong S-L, Tang M-O, Christensen J, Stadler RW, Lau C-P. Intrathoracic impedance monitoring in patients with heart failure. Circulation. 2005; 112:841–848. [PubMed: 16061743]
17. Abraham WT, Compton S, Haas G, Foreman B, Canby RC, Fishel R, McRae S, Toledo GB, Sarkar S, Hettrick DA. FAST Study Investigators: Intrathoracic impedance vs daily weight monitoring for predicting worsening heart failure events: results of the Fluid Accumulation Status Trial (FAST). Congestive Heart Failure. 2011; 17:51–55. [PubMed: 21449992]
18. Bourge RC, Abraham WT, Adamson PB, Aaron MF, Aranda JJM, Magalski A, Zile MR, Smith AL, Smart FW, O'Shaughnessy MA, Jessup ML, Sparks B, Naftel DL, Stevenson LW. Randomized controlled trial of an implantable continuous hemodynamic monitor in patients with advanced heart failure: The COMPASS-HF Study. J Am Coll Card. 2008; 51:1073–1079.
19. Ritzema J, Melton IC, Richards AM, Crozier IG, Frampton C, Doughty RN, Whiting J, Kar S, Eigler N, Krum H, Abraham WT, Troughton RW. Direct left atrial pressure monitoring in ambulatory heart failure patients. Circulation. 2007; 116:2952–2959. [PubMed: 18056531]
20. Abraham WT, Stevenson LW, Bourge RC, Lindenfeld JA, Bauman JG, Adamson PB. Sustained efficacy of pulmonary artery pressure to guide adjustment of chronic heart failure therapy: complete follow-up results from the CHAMPION randomised trial. The Lancet. 2016; 387:453–461.
21. Cahalin LP, Mathier MA, Semigran MJ, Dec GW, DiSalvo TG. THe six-minute walk test predicts peak oxygen uptake and survival in patients with advanced heart failure. Chest. 1996; 110:325–332. [PubMed: 8697828]
22. Brooks GC, Vittinghoff E, Iyer S, Tandon D, Kuhar P, Madsen KA, Marcus GM, Pletcher MJ, Olgin JE. Accuracy and usability of a self-administered 6-minute walk test smartphone application. Circulation: Heart Failure. 2015; 8:905–913. [PubMed: 26283292]
23. Klein L. Treating hemodynamic congestion is the key to prevent heart failure hospitalizations. JACC: Heart Failure. 2016; 4:345–347. [PubMed: 27126282]
24. Zanetti, JM., Salerno, DM. Seismocardiography: a technique for recording precordial acceleration. Computer-Based Medical Systems, 1991 Proceedings of the Fourth Annual IEEE Symposium; 1991; p. 4-9.
25. Inan OT, Migeotte PF, Kwang-Suk P, Etemadi M, Tavakolian K, Casanella R, Zanetti J, Tank J, Funtova I, Prisk GK, Di Rienzo M. Ballistocardiography and seismocardiography: a review of recent advances. Biomedical and Health Informatics, IEEE Journal of. 2015; 19:1414–1427.
26. Etemadi M, Inan OT, Heller JA, Hersek S, Klein L, Roy S. A wearable patch to enable long-term monitoring of environmental, activity and hemodynamics variables. IEEE Transactions on Biomedical Circuits and Systems. 2016; 10:280–288. [PubMed: 25974943]
27. Steimle AE, Stevenson LW, Chelimsky-Fallick C, Fonarow GC, Hamilton MA, Moriguchi JD, Kartashov A, Tillisch JH. Sustained hemodynamic efficacy of therapy tailored to reduce filling pressures in survivors with advanced heart failure. Circulation. 1997; 96:1165–1172. [PubMed: 9286945]
28. Norman HS, Oujiri J, Larue SJ, Chapman CB, Margulies KB, Sweitzer NK. Decreased cardiac functional reserve in heart failure with preserved systolic function. J Card Fail. 2011; 17:301–308. [PubMed: 21440868]
29. ATS Statement. American Journal of Respiratory and Critical Care Medicine. 2002; 166:111–117. [PubMed: 12091180]

30. Brigham, EO. The fast Fourier transform and its applications. Englewood Cliffs, New Jersey: Prentice Hall; 1988.

31. Jain AKM, Murty Narasimha, Flynn Patrick J. Data clustering: a review. ACM computing surveys (CSUR). 1999; 31:264–323.

32. Bishop, CM. Pattern recognition and Machine Learning (Information Science and Statistics). New York, New York: Springer-Verlag; 2006.

33. Dong, W., Moses, Charikar, Li, Kai. Efficient k-nearest neighbor graph construction for generic similarity measures. Proceedings of the 20th International Conference on World Wide Web (WWW '11); Hyderabad, India. 2011; p. 577-586.

Clinical Perspective

What is new?

- Existing wearable devices are limited to the measurement of actigraphy and electrocardiogram signals, which do not provide actionable information for this patient population.
- This paper describes an initial study where cardiogenic mechanical signals are measured with a wearable patch, and these signals – measured in the context of exercise – are shown to provide discriminative value in terms of assessing the state of heart failure patients.

What are the clinical implications?

- Remote monitoring of heart failure patients at home using wearable devices can allow titration of care and thereby potentially reduce hospitalizations.
- The approach described here can be leveraged in future studies to monitor patients at home, and determine if the measured signals and their associated features extracted using graph mining algorithms can provide specific and sensitive prediction of worsening state and risk of exacerbation.

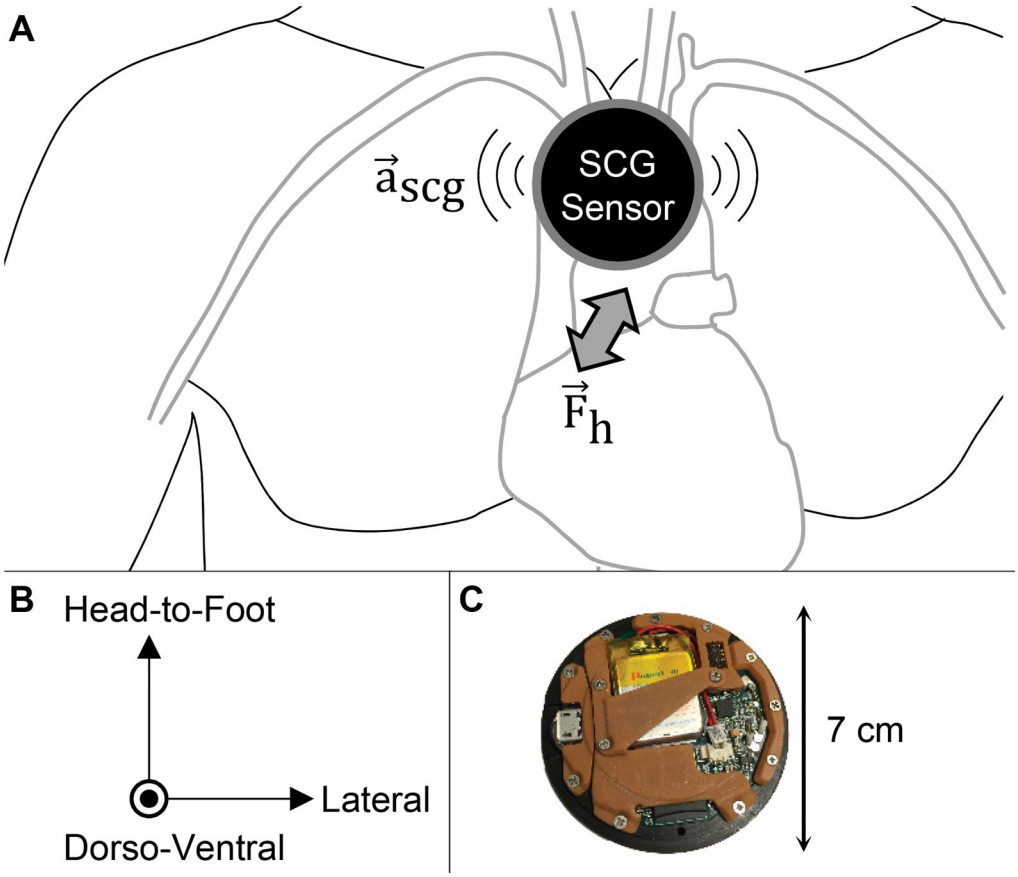

Figure 1. Seismocardiogram and Electrocardiogram Sensing Patch

(a) The seismocardiogram (SCG) signal represents the vibrations of the chest wall in response to the movement of the heart and blood with each heartbeat. SCG is measured using a miniature, three-axis accelerometer, typically positioned on the mid-sternum. (b) The SCG signal consists of vibrations in three-axes: head-to-foot, dorso-ventral, and lateral. (c) A custom, small, wearable patch for measuring SCG and electrocardiogram signals was designed. The patch is placed on the chest using three gel adhesive electrodes, and stores data locally on a micro secure digital (microSD) card. The low power design allows for > 50 hours of continuous recording and use without recharging the battery.

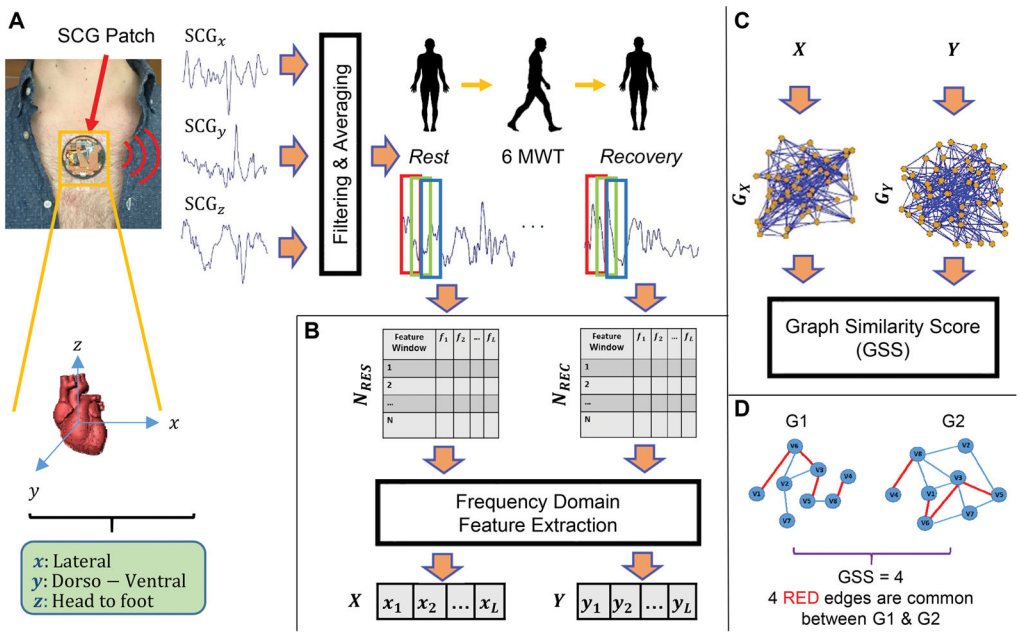

Figure 2. General Overview of the Proposed Method

(a) The SCG signals (three-axes [dorso-ventral, DV, head-to-foot, HF, and lateral, LAT]) of heart are measured using the custom, wearable patch. Filtering is applied and SCG_{3D} (a point-by-point average of the three axes) is calculated. Then, SCG_{3D} of rest and recovery segments are windowed and generate N_{RES} and N_{REC}. (b) The L frequency domain feature sets (***X*** and ***Y***) are computed from N_{RES} and N_{REC}. (c) Two kNNG graphs (G_X and G_Y) are constructed from frequency feature vectors ***X*** and ***Y*** and GSS is calculated to measure similarity in between rest and recovery states. (d) An example of GSS calculation between two illustrative graphs.

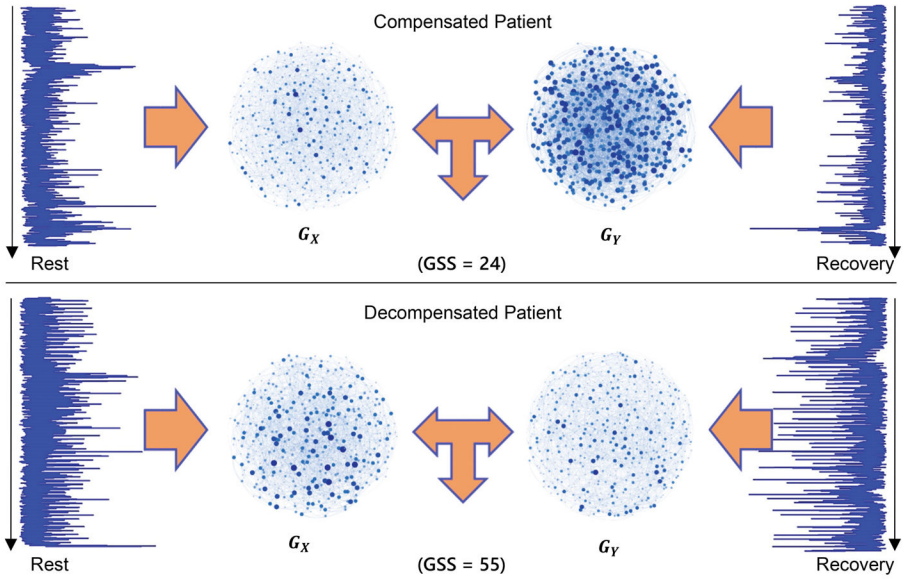

Figure 3. Calculated GSS for Representative Decompensated and Compensated Patients

Representative SCG time traces from rest and recovery following the 6MWT and associated G_X and G_Y graphs of a compensated patient with HF (top) and a decompensated patient (bottom). For the decompensated patient, the GSS value is 55 and for the compensated patient, the corresponding value is 24. This result demonstrates the higher similarity in SCG waveform structure between rest and recovery phases of the decompensated patient in comparison with compensated patient. The graphs also demonstrate the higher similarity for decompensated versus compensated states visually.

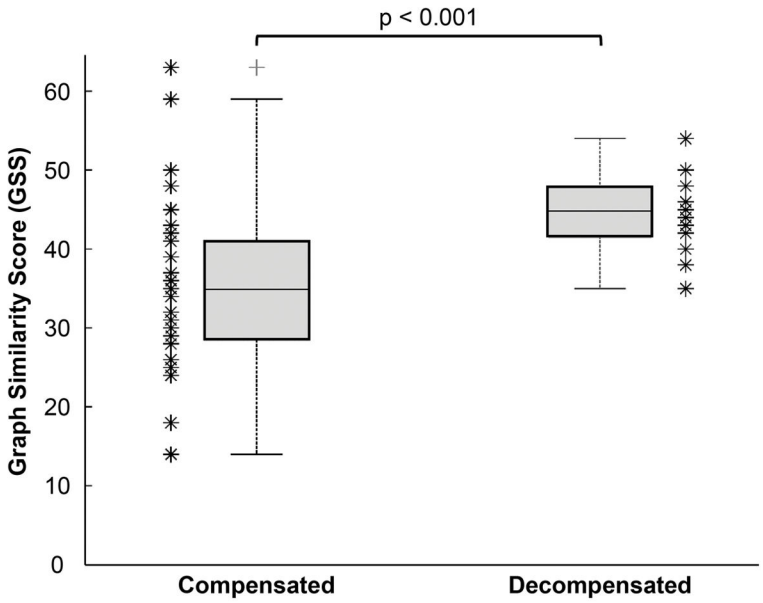

Figure 4. Overall Statistical Analysis of the GSS Metric from All Patients Grouped by Clinical State (Compensated versus Decompensated)

The GSS between rest and recovery phases was significantly higher for the decompensated patients as compared to compensated; n = 45 subjects ($p<0.001$).

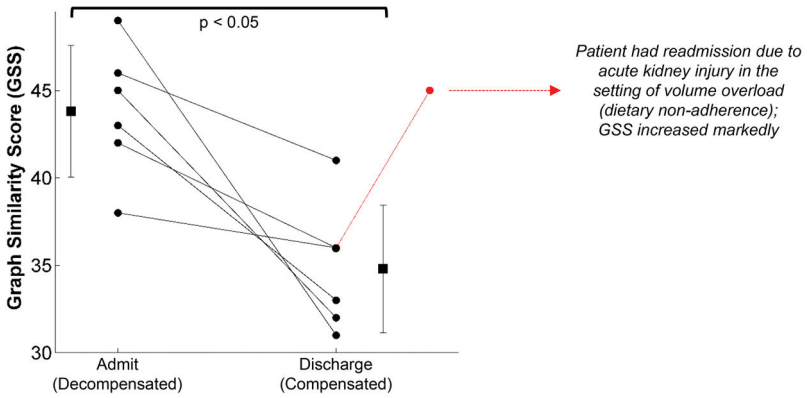

Figure 5. GSS for HF Inpatients Decreases from Admit to Discharge

Longitudinal results from a subset of the inpatient population for which the 6MWT data was obtained when the subjects were admitted (left) and upon discharge (right) following treatment. For all patients, GSS decreased at discharge as compared to when first admitted. Thus, as the decompensated patients were treated, longitudinal changes in the physiological response to exercise were observed in a consistent manner with the cross-sectional data from the overall cohort of subjects. One patient had a third visit as well, and showed markedly increased GSS because of readmission due to acute kidney injury and volume overload.

Table 1

Subject demographics and cardiovascular function parameters for study participants (grouped by decompensated and compensated heart failure patients). Values shown are mean ± standard deviation. Statistical significance between groups in values, where applicable, was evaluated using an unpaired t-test.

	Decompensated (n = 13)	Compensated (n = 32)	*p*-value
Gender	11 (85%) M, 2 (15%) F	22 (69%) M, 10 (31%) F	-
Height (cm)	176.4 ± 12.1	173.1 ± 7.9	0.28
Weight (kg)	93.1 ± 15.3	86.9 ± 21.3	0.35
Age (years)	50 ± 16	57 ± 15	0.17
Ejection Fraction	20 ± 7	33 ± 14	0.003
NYHA Class	1 (8%) III, 12 (92%) IV	4 (12%) I, 12 (38%) II, 9 (28%) III, 7 (22%) IV	-
Dyspnea on exertion (%)	92	50	-
Dyspnea at rest (%)	77	31	-
Orthopnea > 2 pillows (%)	92	34	-
Paroxysmal nocturnal dyspnea (%)	69	9	-
Jugular Venous Pressure (cmH_2O)	14 ± 3	8 ± 2	0.0001
Pulmonary rales (%)	92	19	-
S3 present (%)	46	9	-
Bilateral leg edema (%)	69	25	-
Systolic blood pressure (mmHg)	95 ± 15	110 ± 18	0.01
Diastolic blood pressure (mmHg)	65 ± 8	75 ± 14	0.02
Heart Rate (bpm)	95 ± 16	77 ± 16	0.001
Pulmonary edema on chest X-ray (%)	69	N/A	-
BNP (pg/mL)	4760 ± 450	380 ± 102	0.0001
Furosemide (mg/day)	240 ± 40	80 ± 20	0.0001
Angiotensin converting enzyme inhibitors/receptor antagonists (%)	92	100	-
Beta-blockers (%)	77	90	-
Mineralocorticoid receptor blockers (%)	77	100	-